

Magnetic dichroism in valence-band photoemission from Co/Cu(001): Experiment and theory

A. Fabelsa and E. Kisker

Institut für Angewandte Physik, Universität Düsseldorf, D-40225 Düsseldorf, Germany

J. Henk and R. Feder*

Theoretische Festkörperphysik, Universität Duisburg, D-47048 Duisburg, Germany

(Received 27 November 1995; revised manuscript received 26 February 1996)

Ferromagnetic Co films on Cu(001) have been investigated both experimentally and theoretically by photoemission from valence bands with unpolarized 21.2 eV radiation. The measured spectra exhibit sizable magnetic dichroism and are well reproduced by their counterparts calculated by means of a fully relativistic Green's function method. Prominent intensity maxima can be attributed to direct bulk interband transitions. Magnetic dichroism with unpolarized light is explained by the interplay of exchange splitting with a spin-orbit-induced spin-polarization effect for off-normally incident p -polarized light. Experiment and calculations further give evidence that in Co films on Cu(001) prepared at elevated temperatures (400 K), Cu has diffused to the top of the film. [S0163-1829(96)01228-3]

I. INTRODUCTION

In recent years, an effect which has been known for more than a century attracted much interest due to its rich physical information and its application in imaging and analyzing of surfaces: dichroism, in the sense of selective absorption of light in two different (often orthogonal) polarization states, was described by Pasteur.¹ In photoelectron spectroscopy from nonmagnetic solids, dichroism is the difference between electron emission intensities for two orthogonal light-polarization states, for example, left- and right-handed circular polarized light (circular dichroism in angular distribution)² or two perpendicular states of linear polarization.³

For magnetic materials, especially crystalline surfaces and thin films, dichroism was found by changing, in particular reversing, the direction of the magnetization. First observed in absorption experiments with linear⁴ and circular⁵ polarized light, it was subsequently also found in photoelectron emission.⁶ The intensity of the photocurrent changes upon reversal of the light helicity or reversal of the magnetization direction, both of which are macroscopic and easily controllable parameters. For special geometries, reversal of the light helicity is, in fact, equivalent to the reversal of the magnetization, as is obvious from symmetry considerations.

Magnetic dichroism also shows up in photoemission by linear polarized light [magnetic linear dichroism in angular distribution (MLDAD)]. For s -polarized incident light, the two magnetization directions were chosen perpendicular to each other,⁷ for off-normally incident p -polarized light antiparallel.⁸ Since unpolarized light can be viewed as an incoherent superposition of s - and p -polarized light, the latter case implies that at off-normal incidence, even unpolarized light produces magnetic dichroism.⁹ We would like to mention that magnetic dichroism obtained by the reversal of the magnetization is more general than that obtained by switching between two orthogonal states of light polarization, which becomes obvious when considering magnetic dichroism by unpolarized light.

Up to now, most of the experiments focused on core levels, on the one hand angle integrated to obtain sum rules,¹⁰ and on the other hand angle resolved in order to obtain the angular distribution of photoelectrons and the magnetic domain structure.^{11,12} Valence-band measurements of magnetic dichroism have been performed using circular polarized,^{13,14} linear polarized,¹⁵ and even unpolarized^{9,16} light.

On the theoretical side there were several efforts to explain magnetic dichroism. Cherepkov,¹⁷ as well as Thole and van der Laan,¹⁸ developed atomic models, which successfully describe qualitatively and semiquantitatively experimental data obtained from core levels. One picture for explaining magnetic dichroism in photoemission is interference of final-state partial waves combined with spin-orbit coupling (SOC) in the initial states.¹⁹ Tamura *et al.* calculated core-level emission spectra for semi-infinite crystals within the relativistic layer-KKR framework,²⁰ taking the final state correctly as time-reversed low-energy electron-diffraction (LEED) state. Recent experiments revealed limitations of atomic models, which were attributed to scattering of the outgoing electron.^{16,21} In other words, the crystal structure has to be taken into account in theory.²² For valence-band photoemission from clean surfaces and thin films, relativistic layer-KKR calculations within the one-step model were done by Feder and co-workers.^{23–26} In this work, the structure and symmetry of the entire system (semi-infinite solid, incident light, and magnetization) were fully taken into account. In general, magnetic dichroism occurs if a photoelectron spin-polarization component parallel to the magnetization is produced by SOC. This more fundamental picture — since it holds for both core levels (as long as the one-particle picture applies) and valence bands — is based on analytical calculations of the photoelectron spin-density matrix within the one-step model²⁷ and confirmed by numerical relativistic calculations (cf., for example, Refs. 23 and 24).

In this paper, we present a joint experimental and theoretical investigation of magnetic dichroism in photoemission from valence bands. As a prototype system, we chose fcc-Co films on Cu(001), which has been intensively studied in the

literature.²⁸ Our aims are to explain the magnetic dichroism in angular distribution (MDAD) by unpolarized light and to obtain information on the electronic structure of fcc-Co(001) by comparing experimental and theoretical photoemission spectra.

This paper is organized as follows. In Sec. II, we give a brief survey of the experimental apparatus and the setup. In Sec. III, we outline essential theoretical ingredients. In Sec. IV, the origin of the MDAD for unpolarized light is revealed by symmetry arguments and some symmetry relations of the photoelectron spin polarization vector are derived. Experimental and theoretical results are presented and discussed in Sec. V.

II. EXPERIMENTAL DETAILS

Cobalt films were deposited on a Cu(001)-single crystal at substrate temperatures of $T=300$ K and $T=400$ K, from a Co rod with 99.99% purity heated by electron bombardment. The deposition rates were kept constant at 0.5 ML/min, as calibrated by a quartz microbalance. Since the layer-by-layer growth of this system below 450 K is well known (see for example Ref. 29), the ML thickness could be easily concluded from the deposition time. The fcc structure of the Co films was confirmed by LEED, which also yields the definition of the surface normal. From threshold photoemission measurements, the work functions were determined as 4.54 eV for Cu(001) and 4.96 eV for 20 ML of Co on Cu(001). This allowed a determination of the vacuum level and hence a direct comparison with theoretical data.

All photoemission measurements were done at room temperature. Photoelectrons were excited by unpolarized VUV radiation from a resonance lamp (photon energies He_I: 21.22 eV, He_{II}: 40.81 eV) and detected by a hemispherical analyzer with a radius of 150 mm (VSW150). The electrons were collected with about 5° full acceptance at a pass energy of 1 eV, which leads to an apparatus energetic resolution (37 meV), which is small compared to the thermal broadening of the spectra (114 meV). The geometry of the experiment is shown in Fig. 1. The easy axis of the magnetization \vec{M} is the [110] direction (x axis). The direction of light incidence was dictated by our present apparatus: plane of incidence at $\varphi=135^\circ$ relative to \vec{M} and polar angle $\vartheta=60^\circ$ relative to the surface normal. We note that while magnetic dichroism should be maximal for $\varphi=90^\circ$ and a somewhat smaller value of ϑ , it turns out to be still appreciable in the present geometry.

The experimental photoemission spectra have been recorded by repeated cycles of sampling the photoelectrons (one sweep over the kinetic-energy range), reversing the magnetization direction by flashing, subsequent sampling (also one sweep), and flashing. Because both the photon flux and the sampling time per energy are constant, the intensities for $+\vec{M}$ and $-\vec{M}$ are directly comparable and the asymmetry can be calculated correctly.

III. THEORETICAL APPROACH

Spin- and angle-resolved photoemission spectra from the semi-infinite crystalline system, bulk band structure, and layer density of states (LDOS) are calculated simultaneously

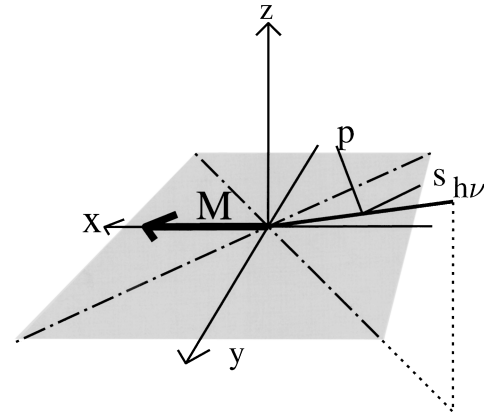


FIG. 1. Experimental setup for MDAD measurements from fcc-Co(001) in normal emission. Unpolarized light with photon energy $h\nu$ impinges at a polar angle of 60° with respect to the surface normal (z axis, [001] direction) and an azimuth of 135° with respect to the magnetization M (parallel to the x axis, [110] direction) onto the solid surface (gray area). The electric-field vectors of p -polarized and s -polarized partial waves are shown in addition, (p,s) . Traces of fcc(001)-mirror planes are the x and the y axes, as well as the two dashed-dotted lines.

within a relativistic layer-KKR-type Green's function formalism, which has recently been presented in detail.³⁰ We employ an effective quasiparticle potential of muffin-tin shape, which has been calculated self-consistently for bulk-fcc-Co with Cu lattice constant. Electron and hole lifetimes are incorporated via a uniform imaginary (absorptive) self-energy part, for which we assume an energy-dependent form suggested and successfully applied to Ni(111) by Gollisch and Feder.³¹ Specifically, we choose $\text{Im}\Sigma=0.38(E-E_F)^{1.59}$, which considerably suppresses emission from the majority d bands below -1 eV. The other parameters are the same as in Ref. 25.

Although experimentally we have a Co film of 20 ML thickness on a Cu(001) substrate, we use for the comparison theoretical results obtained for semi-infinite Co(001) (with appropriate lattice constants). This is justified by the fact that the film is thick enough to suppress emission from the copper substrate. Calculated photoemission spectra for the Co/Cu-film system are almost identical to those for semi-infinite Co(001), except for minor intensity modulations near E_F , due to quantum well states ("film states"), which are hardly resolved in the present experiment.

The geometrical structure of Co films on Cu(001) has been intensively studied by LEED analysis.^{32,33} For a Co film of 8 ML thickness, Clarke *et al.*³² found that lowest reliability factors are obtained for a fct structure with relaxation of the outermost layer (d_{12} reduced by 6%, with respect to the Cu interlayer spacing) and a contraction of the Co interlayer distance (d reduced by 3%). We have used this "best fit" geometry in our calculations, but have additionally investigated how the magnetic dichroism (asymmetry) and the surface electronic structure are affected by surface structural details. Obviously, the energies of surface states and resonances near the Fermi level depend rather strongly on the position of the surface potential barrier. Further, a contraction of the outermost interlayer distance (d_{12}) is nec-

essary to obtain majority spin surface resonances at about 0.5 eV below the Fermi energy.

Finally, we note that the present calculations, which require perfect lattice periodicity parallel to the surface, are rigorously valid only for zero temperature, whereas the experimental data were taken at room temperature. Besides excitation of phonons, elevated temperatures imply fluctuations of the local spin magnetic moments. These produce strong effects in room temperature photoemission from ultrathin films,³⁴ for which the Curie temperature is rather small (several hundred K)³⁵ compared to the Co bulk value (1388 K). For films of 20 ML thickness, however, we expect the effect of spin fluctuations on the photoemission results to be very small, since the Curie temperature is close to that of bulk Co.

IV. MAGNETIC DICHROISM WITH UNPOLARIZED LIGHT

In this section, we elucidate the origin of magnetic dichroism with unpolarized light. First, some symmetry arguments will be given, then we report briefly on recent analytical results on MLDAD in normal emission.

In the (hypothetical) nonmagnetic case, Co(001) shows $4mm$ symmetry (C_{4v} in Schönflies notation), which consists of a fourfold rotational axis, e.g., the surface normal (z axis), and two sets of perpendicular mirror planes. Each set is rotated by 45° , with respect to the other (cf. Fig. 1). In the ferromagnetic case with in-plane magnetization, this symmetry is reduced to $2\bar{m}m$ (bars indicate the additional operation of time reversal) if the magnetization \vec{M} lies within a mirror plane, for example, in the $[110]$ direction (easy axis, denoted as x axis). Therefore, the electronic states cannot be classified by the irreducible representations Δ_6 and Δ_7 of the double group associated with $4mm$. Instead, there are two one-dimensional and degenerate by time-reversal representations,³⁶ γ_1 and γ_2 , the basis functions of which are closely connected to those of the double group $2mm$ (cf. Ref. 27). Each basis set consists of functions with spin parallel and antiparallel to \vec{M} . Thus, the spin expectation value of a band may vary continuously between -1 and $+1$.

Unpolarized light impinging on the (001) surface can be described as an incoherent superposition of an s - and a p -polarized light electromagnetic wave. Therefore, the photoemission intensity is the sum of the intensities obtained for s - and p -polarized light: $I(\pm\vec{M}, \text{unpol.}) = I(\pm\vec{M}, s) + I(\pm\vec{M}, p)$. Let us consider the effect of the operations E (trivial operation), m_x [reflection at the (y, z) plane], m_y [reflection at the (x, z) plane], and C_2 (rotation around the surface normal by 180°) of the symmetry group $2mm$ on the electric field vector \vec{E} , the spin-polarization vector \vec{P} of the photoelectron, and on the magnetization M along the x axis (cf. Table I).

For s -polarized light ($E_z=0$), we obtain for $E_y=0$ or $E_x=0$ that $P_y=P_z=0$ and P_x changes sign if M is reversed (cf. operation C_2 in Table I). Obviously, there is no MLDAD. For $E_x \neq 0$ and $E_y \neq 0$, we find that all three components of \vec{P} may be nonzero. The in-plane components change sign if M is reversed, but P_z does not. This is completely in line with the recently theoretically predicted³⁷ and experimentally confirmed³⁸ linear spin polarization effect

TABLE I. Effect of the symmetry group $2mm$ on the electric-field vector $\vec{E}=(E_x, E_y, E_z)$, the photoelectron spin-polarization vector $\vec{P}=(P_x, P_y, P_z)$, and the magnetization M along the x axis (cf. Fig. 1).

Operation	Electric-field vector	Polarization	Magnetization
E	(E_x, E_y, E_z)	(P_x, P_y, P_z)	M
m_x	$(-E_x, E_y, E_z)$	$(P_x, -P_y, -P_z)$	M
m_y	$(E_x, -E_y, E_z)$	$(-P_x, P_y, -P_z)$	$-M$
C_2	$(-E_x, -E_y, E_z)$	$(-P_x, -P_y, P_z)$	$-M$

(LSPE) for (110) surfaces of nonmagnetic cubic crystals.

We now turn to off-normal incident p -polarized light ($E_z \neq 0$). For $E_y=0$, i.e., \vec{E} and \vec{M} are coplanar, we find that there is no MLDAD (cf. operation m_y). For $E_x=0$, however, i.e., \vec{E} and \vec{M} are orthogonal, there is no operation, which turns \vec{M} into $-\vec{M}$ and simultaneously \vec{E} into $\pm\vec{E}$. Thus, there is a MLDAD. This statement holds also for arbitrary azimuth, i.e., for $E_x \neq 0$ and $E_y \neq 0$. Further, all three components of \vec{P} may be nonzero.

The above symmetry arguments are supported by analytical calculations of the photoelectron spin-density matrix,²⁷ which reveal that there is a MLDAD by off-normal incident p -polarized light if there is a component of \vec{P} parallel to \vec{M} brought about by SOC in the nonmagnetic limit. In the expression for the photoemission intensity, there are two terms. The first remains unchanged if \vec{M} is reversed and does not vanish in the nonmagnetic limit. The second one changes sign by the reversal of \vec{M} and vanishes in the nonmagnetic limit (where obviously there is no magnetic dichroism). Corresponding terms occur in the expression for the component of the spin polarization parallel to \vec{M} . But here, the first term changes sign by reversal of \vec{M} and vanishes in the nonmagnetic limit. The second term does not change sign and remains in the nonmagnetic limit. In other words, this term is exclusively due to SOC and is, therefore, connected to the well-known spin-polarization effect for off-normal incident p -polarized light, which has been theoretically predicted by Tamura *et al.*³⁹ and experimentally confirmed.⁴⁰

From the experimental point of view, measurements with unpolarized light are advantageous with respect to conventional MLDAD experiments. Due to the high photon flux, which is considerably reduced by a polarizer in MLDAD, high count rates can be obtained. The asymmetry for unpolarized light, which is defined by

$$A(\text{unpol.}) = \frac{I(+M, p) - I(-M, p)}{I(+M, s) + I(+M, p) + I(-M, s) + I(-M, p)} \quad (1)$$

is reduced with respect to the standard MLDAD case (off-normal incident p -polarized light), because the s -polarized part of the unpolarized light produces no MLDAD in the chosen setup, i.e., $I(+M, s) = I(-M, s)$.

In conclusion, the MDAD for unpolarized light, denoted UMDAD by Getzlaff *et al.*,⁹ is a straightforward consequence of the MLDAD in standard geometry, i.e., by off-

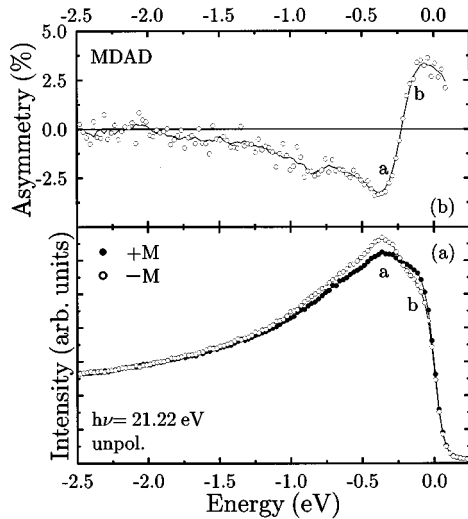


FIG. 2. Experimental MDAD of 20 ML Co/Cu(001) taken at 21.22 eV photon energy with unpolarized light (incident off normal as specified in Fig. 1) in normal emission. The sample has been prepared at room temperature. (a) Solid (dotted) circles represent spectra for magnetization in $[110]$ direction ($[\bar{1}\bar{1}0]$ direction); (b) corresponding asymmetry. Maxima discussed in the text are labeled a and b . The energy zero is the Fermi level.

normal incident p -polarized light with the electric-field vector having no component in the direction of the magnetization.

V. RESULTS AND DISCUSSION

In this section, we present experimental and numerically calculated results on photoemission intensity and MDAD spectra with unpolarized light for ferromagnetic Co on Cu(001).

A. MDAD for 300 K films

We begin with experimental data for 20 ML Co on Cu(001) prepared at room temperature. Panel (a) of Fig. 2 shows experimental energy distribution curves (EDC's) obtained with unpolarized light (incident at 60° relative to the surface normal) in normal emission for the two magnetization directions ($\vec{M} \parallel [110]$ and $\vec{M} \parallel [\bar{1}\bar{1}0]$, cf. Fig. 1). The two intensity maxima, the first at 0.35 eV [denoted (a) in Fig. 2], the other at 0.1 eV binding energy (b), are both from Co. Corresponding maxima arise in the very early stage of growth and are well known for ultrathin Co films in the 1 ML – 5 ML range.⁴¹ The thickness of the present film prevents contributions from the Cu substrate. Exchange-split partners of the maxima near the Fermi level are not observed, neither in the intensities nor in the asymmetry.

The asymmetry [cf. panel (b) of Fig. 2] within the energy range from -2 eV up to 0 eV shows a minimum of -3.5% at -0.4 eV (a) and a maximum of 3.5% near the Fermi edge (b). Its shape was found to be qualitatively and quantitatively nearly the same for films from 6 ML up to 35 ML thickness.

To explain the above experimental data, we have calculated photoemission spectra for the above described fct

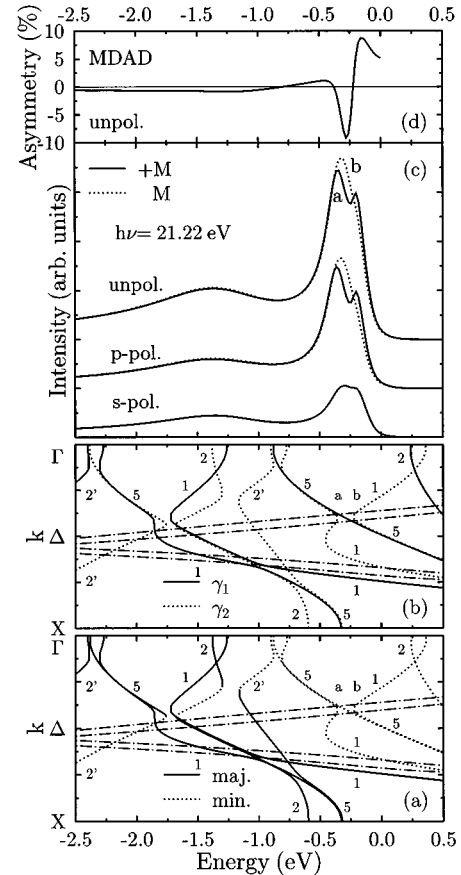


FIG. 3. Theoretical MDAD from Co(001). (a) Relativistic band structure along Γ - Δ - X . Valence bands (for real potential) with majority (minority) spin-polarization expectation value are represented by solid (dotted) lines. The numbers at various parts of the bands indicate their prominent spatial symmetry according to the single-group $4mm$. The real parts of upper bands (obtained for complex potential) with $\text{Im}k_{\perp} < 0.3 \cdot 2\pi/d$ and prominent Δ^1 spatial symmetry (dash-dotted) are shifted down by 21.22 eV photon energy. Direct transitions discussed in the text are labeled a and b . The energy zero is the Fermi level. (b) Band structure as in (a), but with valence bands distinguished according to the relativistic magnetic symmetry types γ_1 (solid lines) and γ_2 (dotted lines). (c) Photoemission intensity for s -polarized, p -polarized, and unpolarized light for magnetization \vec{M} parallel ($+M$, solid) and antiparallel ($-M$, dotted) to $[110]$. Spectra for unpolarized light correspond to the experimental ones shown in Fig. 2. a and b label maxima corresponding to direct transitions. (d) Asymmetry obtained from the spectra for unpolarized light indicating MDAD.

Co(001) in the experimental setup together with the bulk band structure, which turns out to be useful for the interpretation of the spectra. In panel (a) of Fig. 3, we display the relativistic band structure of ferromagnetic fct Co(001) with valence bands distinguished according to predominant majority and minority spin character. In panel (b) we present, less conventionally, the same bands characterized by their magnetic double-group symmetries γ_1 and γ_2 . Although the commonly used classification of the bands by single- or double-group representations of the group $4mm$ does not hold strictly, it is still meaningful to indicate the prominent spatial symmetry of the electronic states in each band (with ‘1’ standing for the single-group representation Δ^1 , etc). In

the valence-band structure, there are numerous SOC-induced splittings and gaps of about 0.1 eV, for example at Γ , and halfway along $\Gamma-X$ around -0.25 eV and -1.2 eV. The latter example can be viewed as an avoided crossing between a majority and a minority band, with the spin-polarization expectation value along the “new” bands going through zero and changing sign. Around -0.25 eV, where nonrelativistically there is a crossing between a minority Δ^5 and a minority Δ^1 band, SOC leads to a γ_1 band with mainly Δ^5 spatial symmetry and two γ_2 bands with both spatial symmetry types, which have equal weights at the hybridization gap. In photoemission by p -polarized light, such hybridization leads, for nonmagnetic crystals, to photoelectron spin polarization, and, for ferromagnets, to magnetic dichroism, as we shall discuss in detail below. The exchange splitting — which is readily visible in the spin-classified presentation in panel (a) of Fig. 3 — depends on the spatial symmetry of the bands and on k_{\perp} . The Γ^{12} ($\Gamma^{25'}$) points are split by 1.62 eV (1.50 eV), for both the X^2 and X^5 points we obtain 1.69 eV splitting. We note that Clemens *et al.* report an average exchange-splitting of (1.55 ± 0.15) eV,⁴² which agrees with our calculated values. This casts doubt on the averaged exchange-splitting value of 1.2 eV, deduced by Mankey *et al.*⁴³ in an experimental inverse photoemission and UV-photoemission investigation.

The calculated photoemission spectra [see panel (c) in Fig. 3] are dominated by two peaks a and b at -0.35 eV and -0.20 eV, respectively. As is seen from the corresponding crossing points between initial and final state bands, these peaks can clearly be attributed to direct transitions from γ_1 initial states, which have dominant spatial symmetry Δ^5 , and from γ_2 states, which are strongly hybridized by SOC in the vicinity of the band gap around -0.25 eV. The energy splitting of peaks a and b , observable with s - and with p -polarized light, directly reflects the spin-orbit splitting of the γ_2 initial band. Both peaks correspond very well to those observed, with unpolarized light, in experiment (cf. Fig. 2). In the energy range from -1.7 eV up to -1.0 eV, there is a broad maximum that is due to emissions from majority bands. Due to the imaginary part of the hole self-energy, which increases rapidly with binding energy and is about 0.7 eV at -1.5 eV, this maximum is much broader than those closer to the Fermi energy. It appears not to be clearly related to direct transitions from our valence bands. This is, however, not surprising, since we included the above-mentioned large imaginary self-energy part in the photoemission calculations (to make them more realistic) but neglected it, for clarity’s sake, in the band-structure calculation. In the experimental data, this maximum is further broadened so that it can hardly be identified.

Magnetic dichroism can be seen in Fig. 3 as the difference between the spectra calculated for $+M$ and $-M$. For s -polarized incident light, there is no MLDAD, in line with the symmetry arguments in Sec. IV. For off-normal incident p -polarized light, however, there is a pronounced MLDAD around -0.25 eV. This is precisely the energy range, in which the γ_2 bands exhibit the SOC-induced gap and the γ_2 initial states comprise Δ^1 and Δ^5 spatial symmetry parts with comparable weights, as already discussed above. This hybridization, which already in the nonmagnetic limit produces photoelectron spin polarization, is ultimately respon-

sible for the observed MLDAD. A change of the photon energy shifts the initial state energies away from the hybridization region and thence reduces the MLDAD. Thus, MDAD measurements can directly reveal SOC-induced hybridization in the initial states.

Unpolarized light can be viewed as an incoherent superposition of s - and p -polarized light. Therefore, EDC’s for unpolarized light can be obtained by summing up the intensities for both linear polarizations. Since the spectra for s -polarized light show no MLDAD, the asymmetry is reduced with respect to that obtained by p -polarized light. Around -0.25 eV the reduction is about 40%. For comparison, in core-level photoemission, the reduction should theoretically be exactly 50% and independent of the energy if the crystal structure is neglected.⁹ The asymmetry for the EDC’s for unpolarized light shows the typical minus/plus structure near the Fermi level, as it is observed in experiment. At energies below -1 eV, the asymmetry is negative and nearly constant, which also corresponds well with the experimental findings. The theoretical asymmetry exceeds the experimental one, due to the experimental resolution and the inelastic background, which are not included in our calculations. In experiment, the polar angle of light incidence (60°) is fixed, but it is close to the angle of maximum asymmetry obtained by theory (51.5°).

Experimental spectra taken with He_{II} photon energy (40.81 eV, not shown here) show no considerable asymmetry ($A < 0.1\%$). Further, the shape of the spectra does not change considerably with respect to those taken at 21.22 eV. Theoretical calculations confirm the experimental results and corroborate further the band-structure origin of the MDAD, i.e., hybridization of initial states. Direct transitions, which show up for s -polarized light, occur at about -0.75 eV near Γ (minority spin) and at -0.32 eV at X (majority spin). For p -polarized light, a broad majority maximum around -0.9 eV shows MLDAD. There are no strong direct transitions from hybridization zones of initial states with Δ^1 and Δ^5 spatial symmetry. As the latter is necessary for the MDAD, the asymmetry is very small, which agrees with the experimental findings.

B. Spin polarization

In addition to the above intensity spectra, we have simultaneously calculated the corresponding spectra of the three components of the photoelectron spin-polarization vector. They are all nonzero in the present geometry with \vec{M} not perpendicular to the plane of incidence. The component collinear with the magnetization \vec{M} (along $[110]$, x axis) [see panel (a) in Fig. 4] reflects the spin polarization of the initial states [cf. panel (a) in Fig. 3]. Because for s -polarized light there is no MLDAD in the chosen setup, reversal of \vec{M} only changes sign of this \vec{P} component. For off-normal incident p -polarized light, however, this does not hold because of the MLDAD.

The in-plane component of \vec{P} perpendicular to \vec{M} (along $[\bar{1}10]$, y axis) is nonzero for both s - and p -polarized light, in accordance with Table I. Again, reversal of \vec{M} changes sign for s -polarized light (cf. operation C_2 in Table I). Note that

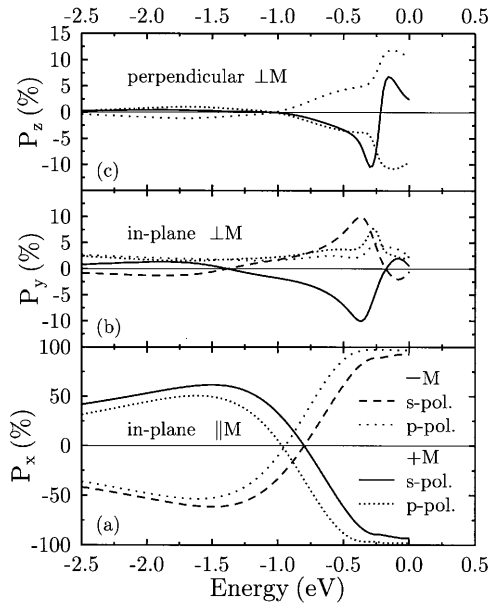


FIG. 4. Theoretical photoelectron spin-polarization vector from Co(001) for s - and p -polarized 21.22 eV light incident at polar angle 60° and azimuthal angle 135° (relative to \vec{M}), calculated for \vec{M} parallel to $[110](+M)$ and reversed $\vec{M}(-M)$ with line symbols as indicated in panel (a): (a) in-plane component $P_{\parallel\vec{M}}$, in the $[110]$ direction; (b) in-plane $P_{\perp\vec{M}}$, in the $[\bar{1}10]$ direction; and (c) normal to surface P_z , in the $[001]$ direction. Note that \vec{M} is not perpendicular to the plane of incidence.

this component is exclusively due to the joint occurrence of exchange and SOC. For p -polarized light, there is no change of sign in the whole initial energy range. In the nonmagnetic limit, this component is also present and due to the LSPE for off-normal p -polarized incident light.

The perpendicular component of \vec{P} (along $[001]$, z axis) for s -polarized light can be attributed exclusively to the LSPE for $2mm$ surfaces. Thus, it does not change with the reversal of \vec{M} , as is shown by the symmetry arguments above (see Table I). For p -polarized light, this component is due to the joint interaction of SOC and exchange.

The \vec{P} components perpendicular to \vec{M} show the largest absolute values in the energy ranges where direct transitions occur, i.e., from -2.0 eV up to -1.5 eV for majority initial states and from -0.5 eV up to 0.0 eV for minority initial states. This further corroborates the band-structure origin of the MDAD.

As has been shown by analytical calculations,²⁷ the expression for the three components of \vec{P} for s - and p -polarized light involves six different combinations of transition-matrix elements. Measurement of the vector \vec{P} for both light polarizations, hand in hand with corresponding calculations, therefore promises to reveal further details of the wave functions.

While experiment and theory are in good agreement with regard to intensities and MDAD, an intriguing discrepancy exists in the photoelectron spin-polarization component along \vec{M} . In the energy range between about -1 eV and E_F , our calculations produce purely minority spin photoelectrons (cf. Fig. 4); spin-resolved measurements (which we

performed for 10 ML and 15 ML Co coverage) reveal a strong majority emission, which significantly exceeds the minority intensity. We can rule out an explanation in terms of the tetragonal distortion of the film, since this has already been taken into account in our calculations. As a possible origin, one may think of surface states or resonances associated with the majority bands at the X point. Such a surface state was suggested to be responsible for a majority peak observed at -0.6 eV by Clemens *et al.*⁴² We, therefore, performed more detailed LDOS calculations varying the surface barrier position and the relaxation of the outermost monolayer. We find two surface resonances that are associated with the majority band edges at the X point (-0.60 eV and -0.32 eV), but the resulting majority contribution to the photocurrent is very small. It seems, however, possible that other DOS contributions could come in due to the disorder of the Co films.

Another mechanism, which we did not take into account in our calculations is the spin dependence of the inelastic mean free path. As was found^{44,45} for Ni, and confirmed also for Fe and Co (see Refs. 46–49 and references therein), the mean free path is significantly larger for majority than for minority electrons. The relative contribution of majority electrons in the observed spin-resolved photocurrent is thence enhanced, provided that there are majority electrons “to start with.” If only minority spin electrons are excited (in a given energy range), only minority electrons reach the detector, regardless of the values of the spin-dependent inelastic mean free paths. By itself, this mechanism can, therefore, not produce majority electrons.

Majority photoelectrons can, however, appear due to spin-flip processes (like excitation of magnons or Stoner pairs), which — in the language of the simple three-step model of photoemission — the photoexcited minority electrons undergo on their way out to the surface. These majority electrons then can benefit from the larger mean free path and contribute relatively more than what is warranted by their creation cross section. A further source of majority electrons can be provided at finite temperatures by small spatial regions of opposite spin polarization generated by spin fluctuations.

In summary, we suggest the following explanation for the observed strong majority spin part of the photocurrent: (1) creation of majority electrons by photoexcitation from surface states or resonances, by spin-flip processes, and possibly by thermal spin fluctuations; (2) subsequent enhancement of their weight (relative to the minority electrons), due to their larger mean free path. Obviously, the interplay of these mechanisms and the resulting spectral strength of the majority emission (quantitatively) depends on the thickness of the Co films. The above explanation in terms of effects, which occur after the actual photoexcitation, which produces MDAD, gains further plausibility from the good agreement that we find between the experimental and the calculated MDAD.

C. MDAD for 400 K films

In Fig. 5, we present experimental photoemission spectra for a sample prepared at $T=400$ K. The most striking departure from the data from the films prepared at room tempera-

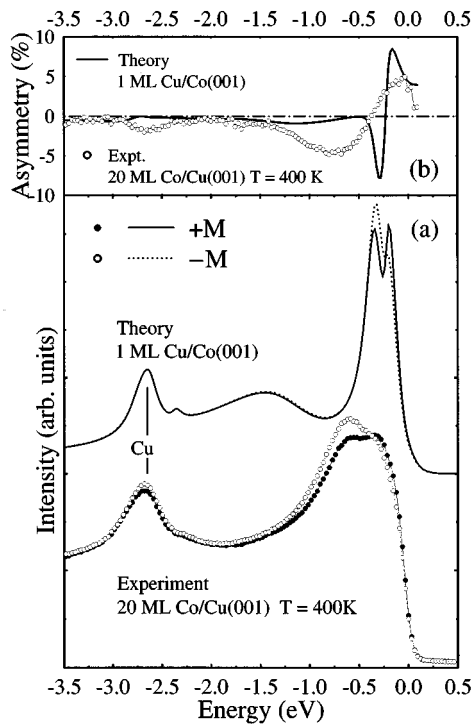


FIG. 5. Normal photoemission from 20 ML Co/Cu(001) taken at 21.22 eV photon energy with unpolarized light. (a) Experimental spectra for magnetization directions $+M$ (filled circles, parallel $[110]$) and $-M$ (outlined circles, parallel $[\bar{1}\bar{1}0]$). The sample has been prepared at 400 K substrate temperature. The theoretical spectra are calculated for 1 ML Cu/Co(001). The Cu peak is marked by lines. (b) Experimental (solid line with dots) and theoretical (solid line) asymmetry for the spectra of panel (a).

ture (cf. Fig. 2) is an additional intensity maximum at -2.65 eV. As preparation of fcc-Co films on Cu(001) at elevated temperatures is known to lead to pin holes⁵⁰ and, therefore, to Cu migration to the top of the Co film, we attribute this additional peak to emission from Cu. Indeed, spectra from clean Cu(001) show a peak at -2.75 eV, which can be interpreted in terms of a bulk interband transition from a mainly Δ^5 -symmetry initial state. The finding that our Cu peak is slightly shifted — by about 0.1 eV towards higher energy — is not surprising, since the initial Cu d state is now localized in the surface region.

Between -1.5 eV and E_F , the intensities and the asymmetry are similar to those in Fig. 2. But the intensity maximum a at -0.35 eV is shifted to -0.55 eV and the associated asymmetry extremum is leftshifted by about 0.2 eV relative to the intensity maximum.

Before trying to explain these changes, we report that even for 35 ML of Co grown at a substrate temperature of 400 K, we find the peak at -2.65 eV. Further, XPS measurements at 1253.6 eV still show a contribution from Cu $2p$ core electrons (which should have an escape depth of about 8 ML). This further corroborates that Cu diffuses onto the surface. This behavior was also found by Li and Tonner⁵¹ with angle-resolved x-ray photoemission spectroscopy. In the LEED pattern, however, we observe no change with respect to the samples prepared at room temperature. This suggests that the Cu-enriched surface region has the same geometrical structure.

To understand in more detail the origin of the additional peak at -2.65 eV and the left shift of the Co peak, we performed LDOS and photoemission calculations for a model consisting of 1 ML Cu/Co(001). The results are also presented in Fig. 5. On the grounds of the LDOS, the additional intensity maximum can be clearly attributed to a Cu d state localized in the topmost monolayer. Further, the photoemission intensity for s -polarized light is much larger than for p -polarized light, which indicates a prominent Δ^5 spatial part of this initial state. In contrast to experiment, the calculated Cu peak shows, however, no significant MDAD. We explain this as follows. Necessary for the MDAD are both spin polarization as well as hybridization of Δ^1 and Δ^5 spatial symmetry parts of the initial states. First, the former is rather small for the Cu-film state, which gives rise to the additional peak. Second, there is nearly no hybridization with Co states, as is evident from the LDOS. Therefore, there is no significant MDAD in the theoretical results for 1 ML Cu on Co(001). Figure 5 shows some further discrepancies between calculated and measured spectra: (a) the experimental left shift of the Co peak (relative to the 300 K spectra) is absent in the theoretical intensity curve; (b) the asymmetry line shapes between about -1 eV and E_F are significantly different; and (c) while in the 300 K data an asymmetry extremum coincides with the intensity maximum, it is left shifted by about 0.2 eV in the 400 K data.

From these discrepancies we conclude that the model of 1 ML Cu/Co(001) falls short of representing the actual experimental surface morphology. Some more clues to the latter can be obtained from earlier experimental results,^{52,53} which suggest that in addition to a Cu coverage there is a Cu admixture in the subsurface layers of Co, and that in this alloy each Cu atom adds two electrons, which increase the filling of the d band of Co. The latter finding may explain why the Co peak (which is at -0.35 eV for the 300 K sample) shifts to lower energy relative to the Fermi energy in the experimental 400 K data. Since such alloying is not (and cannot be) included in our calculations, the theoretical intensity curve does not have this shift. Given “alloying-induced” discrepancies between experimental and calculated intensities, agreement can no longer be expected for the asymmetry. Since magnetic dichroism stems from the interplay of spin-orbit coupling and exchange, a substitution of subsurface Co atoms by Cu, which obviously modifies “exchange,” generally will affect magnetic dichroism asymmetry curves. We now return to the above-mentioned displacement of the asymmetry extremum relative to the Co intensity maximum. We first note that a coincidence of an intensity maximum with an asymmetry extremum cannot generally be expected, but is sort of accidental for particular emission conditions (for which particular initial states play a role). This happens for the 300 K data. The absence of this coincidence in the 400 K data is then likely to be due to the modification of the initial states by a Cu admixture in Co layers. Cu in the subsurface region would also contribute to the observed Cu peak. Since there is stronger hybridization between Cu and Co in the initial states, subsurface alloying may also well lead to the observed MDAD in the Cu peak.

Our above findings shed some new light on earlier photoemission data⁵⁴ obtained for Co films on Cu(001) increasing from 1 ML to 20 ML. While the usual bulk Cu peak de-

creased with coverage, a new peak at -2.6 eV emerged and persisted. The energy position of this peak was nearly independent from film thickness and from photon energy. Such behavior is to be expected for a photoemission peak arising from a state localized in a single Cu monolayer like that presented above. We thence conclude that the Co films of Ref. 54 also had Cu at their surfaces.

It is interesting to compare our 400 K results with those of another experiment, in which the growth of Cu on a 20 ML Co film was studied.⁵⁵ Although their Co film was also prepared at 400 K, they did not find any Cu-related feature for the clean Co (only from 1.5 ML Cu coverage upwards). The lower energetic position of their Co peak (compared to ours) is, according to calculations which we carried out, due to a different photon energy (17 eV). It thus appears that the 400 K Co film of Ref. 55 does not have a significant amount of Cu in its surface region. Comparison with our results suggests a delicate dependence of the surface morphology also on details of other preparation conditions than the temperature.

VI. CONCLUSIONS

Magnetic dichroism in valence-band photoemission by unpolarized light has been investigated both experimentally and theoretically for the prototype thin film system fcc-Co/Cu(001). The good agreement of experiment and theory concerning both intensity and asymmetry yields details of the electronic structure and reveals clearly the origin of this magnetic dichroism.

The maxima in the experimental energy distribution curves can be associated with direct transitions, whereas surface resonances do not make any difference in explaining the spectra. Magnetic dichroism is strongest at direct transitions where electronic initial states of Δ^1 and Δ^5 spatial symmetry hybridize, due to spin-orbit coupling. This fact, in conjunction with dipole selection rules, symmetry arguments, and analytical calculations, demonstrates clearly that magnetic dichroism is associated with spin-orbit-induced spin-polarization effects for linear polarized light, which already occur from nonmagnetic solids. If one of these effects produces a photoelectron spin-polarization component along the magnetization direction, magnetic dichroism occurs. Such a polarization component is brought about by off-normal incident p -polarized light, but not by s -polarized light. The pho-

toemission intensity due to the s -polarized light shows no magnetic dichroism, whereas the intensity for p -polarized light does. Since unpolarized light can be viewed as an incoherent superposition of s - and p -polarized light, magnetic dichroism by unpolarized light is thus easily understood.

By symmetry arguments and analytical calculations, we showed further that, in our geometry (with \vec{M} not normal to the plane of incidence), the photoelectron spin-polarization vector may have three nonvanishing Cartesian components, instead of being aligned parallel to the magnetization, as is the case in the absence of spin-orbit coupling. This was confirmed quantitatively by our numerical calculations.

Samples prepared at $T=400$ K show — even at a Co film thickness of 35 ML film — an additional peak at -2.65 eV. Calculations for a 1 ML Cu/Co(001) confirm that this peak can be attributed to emission from Cu d states. There are, however, several discrepancies between experiment and the spectra obtained for this simple model geometry. They can, in a qualitative manner, consistently be explained by assuming substitutional Cu-Co alloying in subsurface layers. In agreement with some earlier results, we conclude that the preparation at elevated temperatures can lead to pin holes and to Cu migration to the top of the Co film.

While we obtain good agreement between experimental and theoretical intensity and MDAD spectra, there is a discrepancy with regard to the spin polarization of the photocurrent in the vicinity of E_F : spin-resolved measurements show a dominance of majority photoelectrons, whereas our calculations yield minority electrons. We suggest an explanation of the observed majority emission in terms of spin-flip processes (in the final state) and spin dependence of the inelastic mean free path. To resolve this issue in a quantitative way, however, further experimental and theoretical work is required.

ACKNOWLEDGMENTS

The experimental part of this work was supported by the Deutsche Forschungsgemeinschaft within Project No. SFB 166/G7, its theoretical part by the Bundesministerium für Bildung, Wissenschaft, Forschung und Technologie, Contract No. 05621PGA. We also thank the Ministerium für Wissenschaft und Forschung of the state Nordrhein-Westfalen.

*Corresponding author. Electronic address: feder@uni-duisburg.de

¹L. Pasteur, Ann. Chim. Phys. **24**, 442 (1848).

²G. Schönhense, Phys. Scr. **T31**, 255 (1990).

³N. A. Cherepkov and G. Schönhense, Europhys. Lett. **24**, 79 (1993).

⁴G. van der Laan, B. T. Thole, G. A. Sawatzky, J. B. Goedkoop, J. C. Fuggle, J. M. Esteva, R. Karnatak, J. P. Remeika, and H. A. Dabkowska, Phys. Rev. B **34**, 6529 (1986).

⁵G. Schütz, W. Wagner, W. Wilhelm, P. Kienle, R. Zeller, R. Frahm, and G. Materlik, Phys. Rev. Lett. **58**, 737 (1987).

⁶L. Baumgarten, C. M. Schneider, H. Petersen, F. Schäfers, and J. Kirschner, Phys. Rev. Lett. **65**, 492 (1990).

⁷Ch. Roth, H. B. Rose, F. U. Hillebrecht, and E. Kisker, Solid State Commun. **86**, 647 (1993).

⁸Ch. Roth, F. U. Hillebrecht, H. B. Rose, and E. Kisker, Phys. Rev. Lett. **70**, 3479 (1993).

⁹M. Getzlaff, Ch. Ostertag, G. H. Fecher, N. A. Cherepkov, and G. Schönhense, Phys. Rev. Lett. **73**, 3030 (1994).

¹⁰B. T. Thole and G. van der Laan, Phys. Rev. Lett. **70**, 2499 (1993).

¹¹F. U. Hillebrecht and W.-D. Herberg, Z. Phys. B **93**, 299 (1994).

¹²C. M. Schneider, Z. Celinski, M. Neuber, C. Wilde, M. Grunze, K. Meinel, and J. Kirschner, J. Phys. Condens. Matter **6**, 1177 (1994).

¹³C. M. Schneider, M. S. Hammond, P. Schuster, A. Cebollada, R. Miranda, and J. Kirschner, Phys. Rev. B **44**, 12 066 (1991).

¹⁴J. Bansmann, M. Getzlaff, C. Westphal, F. Fegél, and G. Schönhense, Surf. Sci. **269/270**, 622 (1992).

- ¹⁵H. B. Rose, Ch. Roth, F. U. Hillebrecht, and E. Kisker, *Solid State Commun.* **91**, 129 (1994).
- ¹⁶A. Fanelisa, R. Schellenberg, F. U. Hillebrecht, and E. Kisker, *Solid State Commun.* **96**, 291 (1995).
- ¹⁷N. A. Cherepkov, *Phys. Rev. B* **50**, 13 813 (1994).
- ¹⁸B. T. Thole and G. van der Laan, *Phys. Rev. B* **44**, 12 424 (1991).
- ¹⁹G. Schönhense, *Vacuum* **41**, 506 (1990).
- ²⁰E. Tamura, G. D. Waddill, J. G. Tobin, and P. A. Sterne, *Phys. Rev. Lett.* **73**, 1533 (1994).
- ²¹D. Venus, L. Baumgarten, C. M. Schneider, C. Boeglin, and J. Kirschner, *J. Phys. Condens. Matter* **5**, 1239 (1993).
- ²²F. U. Hillebrecht, H. B. Rose, T. Kinoshita, Y. U. Idzerda, G. van der Laan, R. Denecke, and L. Ley, *Phys. Rev. Lett.* **75**, 2883 (1995).
- ²³T. Scheunemann, S. V. Halilov, J. Henk, and R. Feder, *Solid State Commun.* **91**, 487 (1994).
- ²⁴J. Henk, S. V. Halilov, T. Scheunemann, and R. Feder, *Phys. Rev. B* **50**, 8130 (1994).
- ²⁵J. Henk, T. Scheunemann, S. V. Halilov, and R. Feder, *Phys. Status Solidi B* **192**, 325 (1995).
- ²⁶S. V. Halilov, J. Henk, T. Scheunemann, and R. Feder, *Phys. Rev. B* **52**, 14 235 (1995).
- ²⁷J. Henk, T. Scheunemann, S. V. Halilov, and R. Feder, *J. Phys. Condens. Matter.* **8**, 47 (1996).
- ²⁸Proceedings of the 14th International Colloquium on Magnetic Films and Surfaces, Dusseldorf, Germany, 1994, edited by G. Bayreuther, E. Kisker, and J. C. S. Kools [*J. Magn. Magn. Mater.* **148** (1995)].
- ²⁹E. Navas, P. Schuster, C. M. Schneider, J. Kirschner, A. Cebollada, C. Ocal, R. Miranda, J. Cerdá, and P. de Andres, *J. Magn. Magn. Mater.* **121**, 65 (1993).
- ³⁰S. V. Halilov, E. Tamura, H. Gollisch, D. Meinert, and R. Feder, *J. Phys. Condens. Matter* **5**, 3859 (1993).
- ³¹H. Gollisch and R. Feder, *Physica B* **161**, 169 (1989); *Solid State Commun.* **76**, 237 (1990).
- ³²A. Clarke, G. Jennings, R. F. Willis, P. J. Rous, and J. B. Pendry, *Surf. Sci.* **187**, 327 (1987).
- ³³J. R. Cerdá, P. L. de Andres, A. Cebollada, R. Miranda, E. Navas, P. Schuster, C. M. Schneider, and J. Kirschner, *J. Phys. Condens. Matter* **5**, 2055 (1993).
- ³⁴D. Reiser, J. Henk, H. Gollisch, and R. Feder, *Solid State Commun.* **93**, 231 (1995).
- ³⁵J. J. de Miguel, A. Cebollada, J. M. Gallego, R. Miranda, C. M. Schneider, P. Schuster, and J. Kirschner, *J. Magn. Magn. Mater.* **93**, 1 (1991).
- ³⁶L. M. Falicov and J. Ruvalds, *Phys. Rev.* **172**, 498 (1968); J. Ruvalds and L. M. Falicov *ibid.* **172**, 508 (1968).
- ³⁷J. Henk and R. Feder, *Europhys. Lett.* **28**, 609 (1994).
- ³⁸N. Irmer, F. Frentzen, S.-W. Yu, B. Schmiedeskamp, and U. Heinzmann, *Verhandl. DPG* **7**, 1573 (1995); and private communication.
- ³⁹E. Tamura and R. Feder, *Solid State Commun.* **79**, 989 (1991); *Europhys. Lett.* **16**, 695 (1991).
- ⁴⁰B. Schmiedeskamp, N. Irmer, R. David, and U. Heinzmann, *Appl. Phys. A* **53**, 418 (1991).
- ⁴¹W. Clemens, E. Vescovo, T. Kachel, C. Carbone, and W. Eberhardt, *Phys. Rev. B* **46**, 4198 (1992).
- ⁴²W. Clemens, T. Kachel, O. Rader, E. Vescovo, S. Blügel, C. Carbone, and W. Eberhardt, *Solid State Commun.* **81**, 739 (1992).
- ⁴³G. J. Mankey, R. F. Willis, and F. J. Himpsel, *Phys. Rev. B* **48**, 10 284 (1993).
- ⁴⁴A. Bringer, M. Campagna, R. Feder, W. Gudat, E. Kisker, and E. Kuhlmann, *Phys. Rev. Lett.* **42**, 1705 (1979).
- ⁴⁵D. P. Pappas, K.-P. Kämper, B. P. Miller, H. Hopster, D. E. Fowler, C. R. Brundle, A. C. Luntz, and Z.-X. Shen, *Phys. Rev. Lett.* **66**, 504 (1991).
- ⁴⁶E. Kisker, W. Gudat, and K. Schröder, *Solid State Commun.* **44**, 591 (1982).
- ⁴⁷M. Getzlaff, J. Bansmann, and G. Schönhense, *Solid State Commun.* **87**, 467 (1993).
- ⁴⁸J. C. Gröbli, A. Kündig, F. Meier, and H. C. Siegmann, *Physica B* **204**, 359 (1995).
- ⁴⁹W. Kuch, M.-T. Lin, K. Meinel, C. M. Schneider, J. Noffke, and J. Kirschner, *Phys. Rev. B* **51**, 12 627 (1995).
- ⁵⁰A. K. Schmid, Ph. D. thesis, Freie Universität Berlin, 1991; and private communication.
- ⁵¹H. Li and B. P. Tonner, *Surf. Sci.* **237**, 141 (1990).
- ⁵²E. Kneller, *J. Appl. Phys.* **33**, 1355 (1962).
- ⁵³S. Mader, H. Widmer, F. M. d'Heurle, and A. S. Nowick, *Appl. Phys. Lett.* **3**, 201 (1963).
- ⁵⁴C. M. Schneider, Ph.D. thesis, Freie Universität, Berlin, 1989.
- ⁵⁵C. Carbone, E. Vescovo, O. Rader, W. Gudat, and W. Eberhardt, *Phys. Rev. Lett.* **71**, 2805 (1993).